

Fig. 5 : Uncorrected distributions in squared transverse momentum for same event samples described in (a). Horizontal error bars indicate the error in  $t$  which results from the 0.001 rad angular error in arm 1.

(RL 16587)

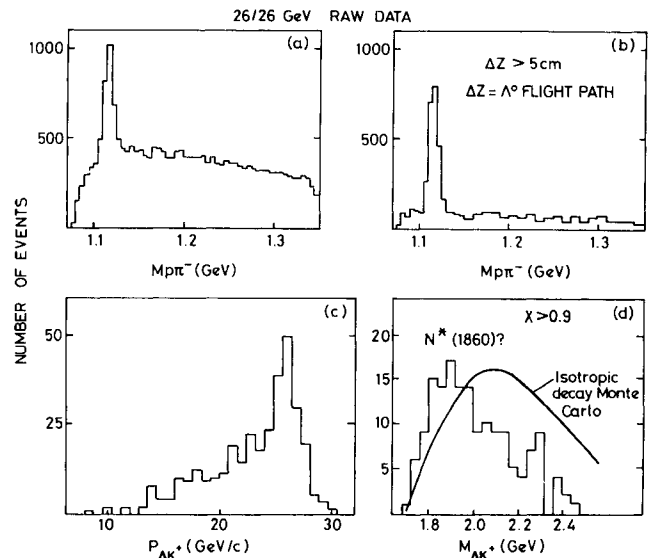


Fig. 6a:  $p\pi^-$  invariant mass spectrum;  
 b: Same but with  $z > 5$  cm (see text).  
 c: Total momentum for  $\Lambda^0 K^+$  system;  
 d: Uncorrected  $M_{\Lambda^0 K^+}$  invariant mass spectrum for  $x > 0.9$ .

(RL 16596)

\*) In striking analogy with the results of the CERN-Holland-Lancaster-Manchester Collaboration in their studies of single diffraction excitation of quasi-elastically scattered protons at the ISR.

\*\*) This result is compatible with earlier results on limiting fragmentation and  $s$ -independence of 2-body correlations by the Pisa-Stony Brook Collaboration at the ISR, see e.g. Phys.Lett.48B, 359 (1974) and earlier results cited therein.

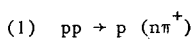
\*\*\*) The detected cross section at each energy is 0.02 mb, corresponding to  $\sigma \sim 0.25$  mb after acceptance correction in the spectrometer if the decay angular distributions are assumed isotropic. Because the internal structure of the  $p\pi^+\pi^-$  system is found to be  $s$ -independent, however, the acceptance corrections do not enter into the cross section ratio.

#### EXPERIMENTAL RESULTS ON INELASTIC DIFFRACTION SCATTERING IN PROTON-PROTON COLLISIONS AT THE ISR

CERN-Hamburg-Orsay-Vienna Collaboration

Presented by C Broll

Experimental data on the reaction



have been obtained using the Split Field Magnet (SFM) detector, complemented with special neutron counters<sup>(1)</sup> at the CERN Intersecting Storage

Rings (ISR). We are reporting on a preliminary analysis of data obtained at  $\sqrt{s} = 53$  GeV; the experiment is continuing and we expect to collect data over the full range of ISR energies,  $\sqrt{s} = 23$  GeV to 62 GeV.

We present here results from 7200 events in terms of four parameters, the four-momentum transfer  $t$ , the invariant mass of  $(n\pi^+)$ , and the polar and azimuthal decay angles in the Jackson frame

$$(2) \quad d^4\sigma/dtdM^*d\phi d\cos\theta$$

Absolute cross sections have been determined by weighting events with a 4-dimensional acceptance table (in terms of  $t, M^*, \phi$  and  $\cos\theta$ ) and with a neutron counter efficiency which had previously been measured<sup>(1)</sup> as a function of neutron energy and impact; an overall factor was applied for normalization. We estimate the absolute scale precision to be  $\pm 20\%$  at present. The  $t$ -dependence of the cross section after integration over all masses and decay angles is shown in Fig. 1. We note the presence of two distinctly different slopes as a dominant feature of the data. The  $t$ -dependence for various regions of mass is shown in the review talk of Didden's.

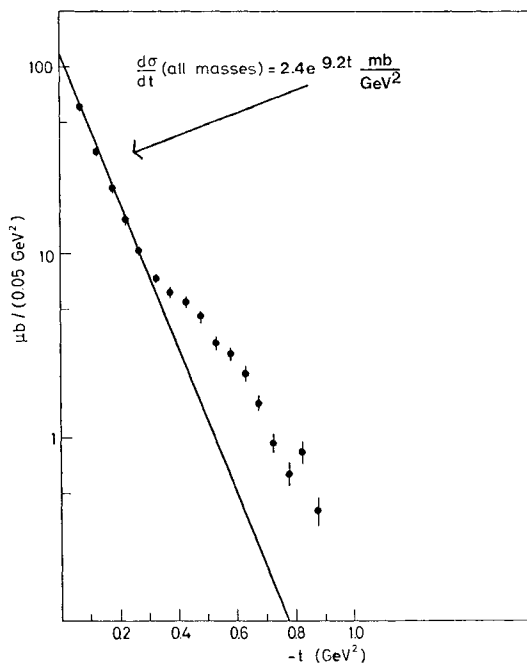


Figure 1. Differential cross section,  $d\sigma/dt$  for the exclusive reaction  $pp \rightarrow p(n\pi^+)$  integrated over  $(n\pi^+)$  invariant mass. (RL 16539)

The  $s$ -dependence of these exponential slopes is shown in Fig. 2 and compared to the slope observed in elastic scattering. We note that all slopes are increasing with  $s$ , at approximately the same rate as in elastic scattering. Shrinkage is a phenomenon shared by elastic and inelastic diffraction scattering.

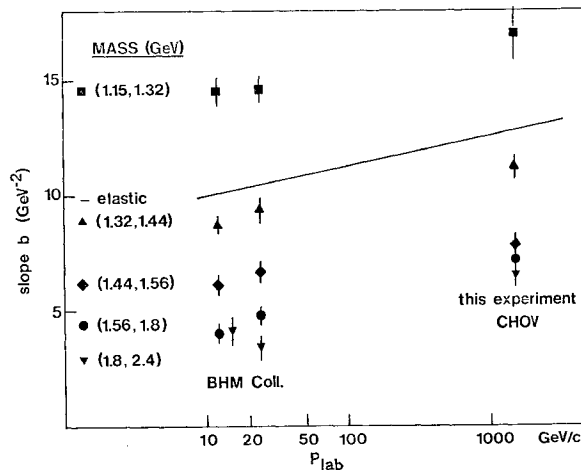


Figure 2.  $s$ -dependence of exponential slope of  $d\sigma/dtdM^*$  in the range  $-t < 0.3 \text{ GeV}^2$  for various mass regions compared to elastic scattering for  $-t < 0.15 \text{ GeV}^2$ . (RL 16538)

There appear to be two distinct components of inelastic diffraction scattering,  $N^*$  production and non-resonant pion production. We expect these components to have different polar angular distributions in the Jackson frame:  $N^*$  resonance production will display forward-backward symmetry, whereas in non-resonant pion production the neutron will be predominantly forward. The corresponding forward-backward asymmetry is indeed observed in the data in Fig. 3 (integrated over all masses and  $-t > 0.05 \text{ GeV}^2$ ). We observe a strong increase of this asymmetry with increasing mass. At mass values above 2.4 GeV diffraction dissociation into the one pion channel is

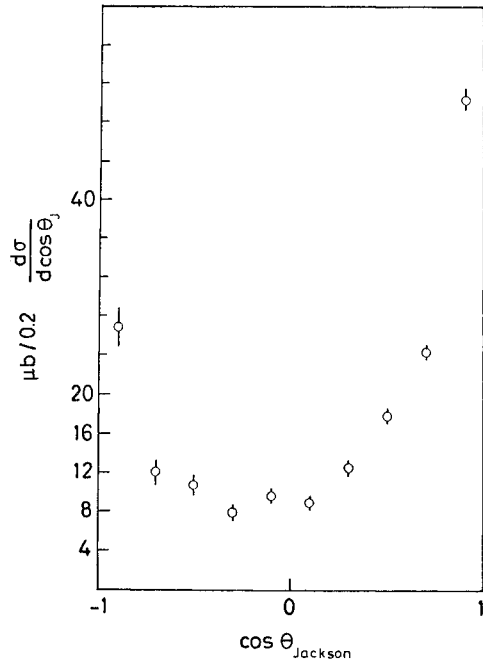


Figure 3. Distribution in polar angle in the Jackson reference frame for all masses. Note the forward-backward asymmetry. (RL 16537)

completely dominated by the non-resonant component. Because of this strong asymmetry it is interesting to compare the mass spectra of events associated with a backward neutron and a forward neutron shown in the talk of Didden's. Selecting a particular mass region around the  $N^*(1688)$ , we note (in Fig. 4) that events in the two hemispheres of the Jackson frame also show distinctly different azimuthal angular dependence. Backward, resonant states seem to decay predominantly perpendicular to the production plane, whereas non-resonant pion production is observed predominantly in the production plane (in analogy to Bremsstrahlung).

We have made an attempt to determine the integrated cross section for reaction (1). Extrapolating  $d\sigma/dt$  in Fig. 1 to  $t = 0$  we find

$$\sigma(pp \rightarrow p n \pi^+) = (270 \pm 80) \mu\text{b}$$

at  $\sqrt{s} = 53 \text{ GeV}$ ; the error contains an estimate of

the scale uncertainty and of the extrapolation uncertainty.

A comparison with lower energy data<sup>(2)</sup> is shown in the review talk of Didden's.

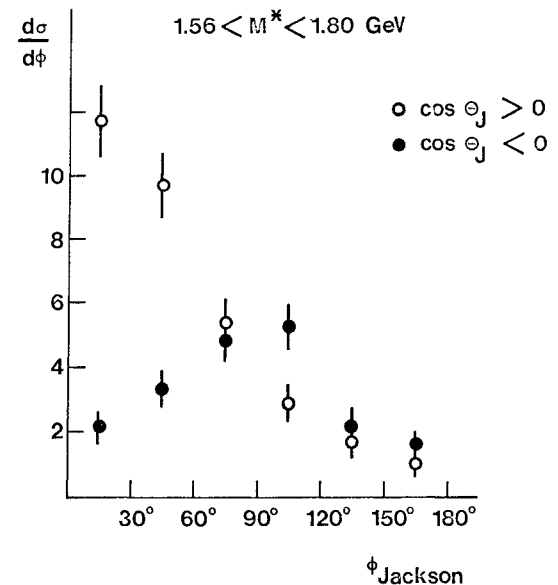


Figure 4. Distribution in azimuthal angle in the Jackson frame of events in the mass region  $1.56 < M^* < 1.80 \text{ GeV}$ . Events in the two hemispheres of the Jackson frame show distinctly different distribution. (RL 16537)

#### References

1. J J Aubert, C Broll, G Coignet, J Favier, L Massonnet, D B Smith, M Vivargent, H Dibon., Preprint IPN, HE 73/03.
2. K Böckmann, et al., Bonn-Hamburg-München Collaboration, Preprint Bonn University PIB 3-27, March 1974